PET imaging of cannabinoid type 2 receptors with [^{11}C]A-836339 did not evidence changes following neuroinflammation in rats

Running head: Imaging CB2R with [^{11}C]A-836339 after neuroinflammation

Geraldine Pottier[1], Vanessa Gómez-Vallejo[2], Daniel Padro[2], Raphaël Boisgard[1], Frédéric Dollé[1], Jordi Llop[2], Alexandra Winkeler[1*], Abraham Martín[4*]

[1.] Imagerie Moléculaire In Vivo, Inserm, CEA, Univ. Paris Sud, CNRS, Université Paris Saclay, CEA - Service Hospitalier Frédéric Joliot, Orsay, France.

[2.] Radiochemistry and Nuclear Imaging, CIC biomaGUNE, Pº Miramon 182, San Sebastian, Spain**.**

[3.] Magnetic Resonance Imaging, CIC biomaGUNE, Pº Miramon 182, San Sebastian, Spain**.**

[4.]Molecular Imaging Unit, CIC biomaGUNE, Pº Miramon 182, San Sebastian, Spain**.**

([*] corresponding authors)

Corresponding authors:

Alexandra Winkeler, Imagerie Moléculaire In Vivo, Inserm, CEA, Univ. Paris Sud, CNRS, Université Paris Saclay, CEA - Service Hospitalier Frédéric Joliot, 4, place du Général Leclerc, 91401 Orsay Cedex (France). *E-mail address*: alexandra.winkeler@cea.fr.

Abraham Martín, Unidad de Imagen molecular; CICbiomaGUNE**,** Edificio Empresarial "C", Pº Miramon 182, San Sebastian, Spain**.** *E-mail address*: amartin@cicbiomagune.es.

Keywords: [^{11}C]A-836339; [^{18}F]DPA-714; PET; cerebral ischemia, neuroinflammation, TSPO, CB2R

ABSTRACT

Cannabinoid type 2 receptors (CB2R) have emerged as promising targets for the diagnosis and therapy of brain pathologies. However, no suitable radiotracers for accurate CB2R mapping have been evidenced so far, limiting the investigation of the CB2 receptor expression using Positron Emission Tomography (PET) imaging. In this work, we report the evaluation of the *in vivo* expression of CB2R with [^{11}C]A-836339 PET after cerebral ischemia and in two rat models of neuroinflammation such as, intrastriatal LPS and AMPA injection. PET images showed a lack of specific [^{11}C]A-836339 in these animal models evidencing the limitation of this radiotracer to image CB2 receptor under neuroinflammatory conditions. Likewise, CB2 receptor displayed a modest expression increase after cerebral ischemia with immunohistochemistry. Finally, the activation of CB2 receptors with the selective agonist JWH133 evidenced a decrease of neuroinflammation by using [^{18}F]DPA-714-PET. Taken together, these findings suggest that [^{11}C]A-836339 is not a suitable radiotracer to monitor *in vivo* CB2R expression by using PET imaging. Future studies will have to investigate alternative radiotracers with higher sensitivity that could provide an accurate binding of CB2 receptor following brain inflammation.

INTRODUCTION

The cannabinoid (CB) receptors are members of a superfamily G-protein coupled receptors involved in a variety of physiological processes including appetite, pain-sensation, mood and memory.[1] The primary receptors of the endocannabinoid system are the CB1 and CB2 cannabinoid receptors.[2] Despite CB1 receptors are predominantly expressed by neurons in the cortex, hippocampus, amygdale, basal ganglia and cerebellum,[3] CB2 receptors are abundant on immune cells regulating migration, cytokine production, and antigen presentation.[4, 5] In the central nervous system (CNS), CB2 receptors have been identified on microglial and dendritic cells evidencing the role of these receptors in CNS inflammatory response.[6, 7] Likewise, several preclinical studies have shown the anti-inflammatory therapeutic potential of CB2 receptor activation in cerebral pathologies such as cerebral ischemia,[8-10] multiple sclerosis,[11, 12] Alzheimer's disease ,[13] Hungtinton's disease,[14, 15] Parkinson's disease [16] and Amyotrophic lateral sclerosis.[17, 18] This therapeutic mechanism responds to the ability of CB2 receptors to attenuate microglial activation and prevent neuronal degeneration in most of the CNS disorders.[2] In this context, the *in vivo* imaging of CB2R with positron emission tomography (PET) might be crucial to further understand the role of these receptors on inflammatory reactions underlying brain diseases. Several PET radiotracers for CB2 receptors have been synthesized and tested in animals, such as [^{11}C]KD2,[19] [^{11}C]RS-016,[20] [^{18}F]CB91,[21] [^{11}C]A-836339 [22] and in human volunteers with [^{11}C]NE40.[23] Among them, [^{11}C]A-836339 has been suggested as a promising radiotracer for the *in vivo* evaluation of a neuroinflammatory reaction in both a systemic lipopolysaccharide (LPS)-induced mouse model of neuroinflammation and a mouse model of Alzheimer's disease.[22] In contrast, [^{11}C]NE40 has not shown to be sensitive enough to visualize the CB2 receptor expression after cerebral ischemia in mice due in part to its low affinity for CB2 receptors.[24] Therefore, the purpose of the present study was to investigate cerebral CB2 receptor changes following neuroinflammatory rat models using PET with [^{11}C]A-836339 and immunohistochemistry. In particular, we were interested in determining the potential of this radiotracer to image CB2 expression following three well established animal models of neuroinflammation such as (i) transient focal cerebral

ischemia[25], (ii) LPS-induced[26] and (iii) α-amino-3-hydroxy-5-methyl-4-isoxazolepropionic acid receptor (AMPA)-induced model in rats.[27] Likewise, [^{18}F]DPA-714, a specific radioligand for the translocator protein 18 kDa (TSPO) and a well known neuroinflammation marker,[28] was used to evaluate the effect of a selective agonist for CB2 receptors (JWH133) on the inflammatory reaction after ischemic stroke in rats. Finally, the neurofunctional outcome was assessed to evaluate the usefulness of the treatment in stroke recovery.

MATERIALS AND METHODS

Animal models

Adult male Sprague-Dawley rats (n=18) for stroke studies and Wistar rats (n=6) for AMPA and LPS administration (300 g body weight; Janvier, France) were used. Animal studies were approved by the animal ethics committee of local authorities and were conducted in accordance with the ARRIVE guidelines and Directives of the European Union on animal ethics and welfare.

Cerebral ischemia and treatment

Transient focal ischemia was produced by a 90 minutes intraluminal occlusion of the middle cerebral artery (MCA) followed by reperfusion as described elsewhere.[29] Briefly, rats were anaesthetized with 2.5% isoflurane in 100 % O_2 and a 2.6-cm length of 4-0 monofilament nylon suture was introduced into the right external carotid artery up to the level where the MCA branches out and animals were sutured and placed in their cages with free access to water and food. After 90 minutes, the animals were re-anesthetized and the filament was removed to allow reperfusion. Six rats were repeatedly examined before (day 0) and at 1, 3, 7, 14, 21 and 28 days after ischemia to evaluate the temporal PET binding of CB2 receptors. The animals studied at day 0 have been considered as the baseline control group. A group of seven rats was inoculated daily for a total of seven days from one hour following MCAO with 0.1 mL JWH133 (in TocriSolve^{TM} 100) (1.5 mg/Kg, i.p.). A control ischemic group of five rats received daily the same volume of vehicle (normal saline). At day seven, treated and control rats were imaged with PET to determine the effect of JWH133 on TSPO expression. In total, MCAO was induced to eighteen rats.

LPS or AMPA administration

Animals were were anaesthetized with 2.5% isoflurane in 100 % O_2 and stereotactically injected with 1 μg lipopolysaccharide (LPS from Escherichia coli 055:B5, Sigma, 1 μg/μL in PBS buffer) (n=4) or 0.5 μL of α-amino-3-hydroxy-5-methylisoxazole-4-propionic acid (AMPA, Sigma, 15 mM) (n=2) using a 1

μL microsyringe (Hamilton) and a micropump (Micro4 Controller; WPI Inc.) into the right striatum (Bregma: +1.0 mm, lateral: -3.0 mm, depth: 4.0 mm from the surface of the brain). The infusion rate was set to 500 nL/min and the syringe was left in place after injection for ten minutes before it was retracted slowly. The site of incision was then cleaned, and sutured using 4.0 braided silk before being disinfected. Animals were maintained normothermic during the surgery through the use of a heating blanket (Homeothermic Blanket Control Unit; Harvard Apparatus Ltd.).

Magnetic resonance imaging

T2-weighted (T_2W) MRI scans were performed in ischemic animals at 24 hours after reperfusion to select the rats (n=6) presenting cortico-striatal lesions to be included in the PET studies. Before the scans, anesthesia was induced with 4% isoflurane and maintained by 2-2.5% of isofluorane in 100% O_2 during the scan. Animals were placed into a rat holder compatible with the MRI acquisition systems and maintained normothermic using a water-based heating blanket at 37ºC. MRI experiments were performed on a 7 Tesla Bruker Biospec 70/30 MRI system (Bruker Biospin GmbH, Ettlingen, Germany), interfaced to an AVANCE III console. The BGA12-S imaging gradient (maximum gradient strength 400 mT/m switchable within 80 μs), an 82 mm inner diameter quadrature volume resonator for transition and surface rat brain coil for reception were used. T2W images were acquired with a RARE sequence with the following parameters: RARE factor 2, TR/TE = 4400/40 ms, FOV = 25 mm x 25 mm, ACQ Matrix =256 x 256, Slice Thickness = 1 mm, 2 averages and 24 contiguous slices. Contiguous slices covering all the infarcted volume were acquired and fat suppression was used.

Radiochemistry

[^{11}C]A-836339 preparation : A-836339 ((Z)-*N*-(3-(2-methoxyethyl)-4,5-dimethylthiazol-2(3H)-ylidene)-2,2,3,3-tetramethylcyclopropanecarboxamide) was labeled by reaction of the corresponding desmethylated precursor with [^{11}C]CH_3I. Carbon-11 was directly generated as [^{11}C]CH_4 in an IBA Cyclone 18/9 cyclotron and transferred to a TRACERlab FX_C Pro synthesis module (GE Healthcare, Waukesha, WI, USA) where [^{11}C]CH_3I was generated via the gas-phase method, distilled under continuous helium flow (20 mL/min) and introduced in a 2 mL stainless steel reaction loop pre-charged with a solution of (Z)-*N*-(3-(2-hydroxyethyl)-4,5-dimethylthiazol-2(3H)-ylidene)-2,2,3,3-tetramethylcyclopropanecarboxamide (1 mg) in dimethylformamide (80 µL) using potassium hydroxide as the base. The reaction was allowed to occur for 5 minutes at 25°C and the crude was then purified by means of high performance liquid chromatography (HPLC) using a Luna C18 column (Phenomenex, Madrid, Spain) as the stationary phase and 0.1M aqueous formic acid solution / methanol 22/78 (v/v) as the mobile phase. The collected fraction (retention time: 9-11 min) was reformulated by dilution with water (20 mL), retention on a C-18 cartridge (Sep-Pak® Light, Waters, Milford, MA, USA) and eluted with ethanol (1 mL) and saline (9 mL). Filtration through a 0.22 µm sterile filter yielded the final injectable solution. For quality control, a Mediterranean Sea18 column (Teknokroma, Barcelona, Spain) was used as stationary phase and 0.1M aqueous formic acid solution / methanol 30/70 (v/v) as the mobile phase. Radiochemical yields and specific activities were 34±4 % (end of bombardment) and 175±8 GBq/µmol at injection time, respectively. Radiochemical purity was >99% in all cases.

[^{18}F]DPA-714 preparation: The synthesis of [^{18}F]DPA-714 (*N,N*-diethyl-2-(2-(4-(2-[^{18}F]fluoroethoxy)phenyl)-5,7-dimethylpyrazolo[1,5-a]pyrimidin-3-yl)acetamide was performed using a TRACERlab FX_{FN} synthesis module (GE Healthcare), based on a one-step procedure, as previously described.[30, 31] Briefly, once transferred into a dedicated (ventilated and lead-shielded) hot-cell, fluorine-18 as [^{18}F]fluoride (cyclotron-produced, IBA Cyclone 18/9) was first trapped on a pre-conditioned Sep-Pak® Accell Plus QMA Light cartridge (Waters, Milford, MA, USA), then eluted from the cartridge with a solution of Kryptofix K2.2.2/K_2CO_3 in a mixture of water and acetonitrile. A solution containing the

appropriate tosyloxy precursor for labelling (*N,N*-diethyl-2-(2-(4-(2-toluenesulfonyloxyethoxy)phenyl)-5,7-dimethylpyrazolo[1,5-a]pyrimidin-3-yl)acetamide, 4 mg) in dimethylsulfoxide (0.7 mL) was added and the mixture heated at 165°C for 5 minutes. The reactor was then cooled at room temperature, the reaction crude diluted with a mixture of acetonitrile and water (2/1, 3 mL), and purified by HPLC using a Nucleosil 100-7 C18 column (Macherey-Nagel, Düren, Germany) as stationary phase and 0.1M aqueous ammonium formate solution (pH = 3.9) / acetonitrile (30/70) as the mobile phase at a flow rate of 7 mL/min. The desired fraction (10-11 min) was collected, diluted with water (20 mL), and the radiotracer was retained on a C-18 cartridge (Sep-Pak® Light, Waters, Milford, MA, USA) and further eluted with ethanol (1 mL). The ethanol solution was finally reconstituted with saline solution (9 mL). Filtration through a 0.22 μm filter yielded the final solution, ready for injection. Radiochemical yields (non-decay corrected) were in the range 8-13% and radiochemical purity was always >95% at the time of injection.

Positron emission tomography scans and data acquisition

Cerebral ischemia studies

PET scans were repeatedly performed before (day 0) and at 1, 3, 7, 14, 21 and 28 days after reperfusion using a General Electric eXplore Vista CT camera (GE Healthcare). Scans were performed in rats anaesthetized with 4% isofluorane and maintained by 2-2.5% of isofluorane in 100% O_2. The tail vein was catheterized with a 24-gauge catheter for intravenous administration of the radiotracer. Animals were placed into a rat holder compatible with PET acquisition system and maintained normothermic using a water-based heating blanket. Animals were subjected to PET scans to assess CB2 receptors ([^{11}C]A-836339) at every time point before and after ischemia onset. For longitudinal imaging evaluation of CB2 receptors, ~70 MBq of [^{11}C]A-836339 were injected concomitantly with the start of the PET acquisition. Brain dynamic images were acquired (24 frames: 1x5, 1x15, 3x30, 5x60, 4x120, 4x180, 6x300 seconds) in the 400-700 keV energetic window, with a total acquisition time of 57.5 minutes. For evaluation of

JWH133 treatment efficacy after ischemia, ~70 MBq of [^{18}F]DPA-714 were injected concomitantly with the start of the PET acquisition and brain dynamic images were acquired for a total of 30 minutes (23 frames 3x5, 3x15, 4x30, 4x60, 4x120, 5x180 seconds). After each PET scan, CT acquisitions were also performed (140 μA intensity, 40 kV voltage), providing anatomical information of each animal as well as the attenuation map for the later image reconstruction. Dynamic acquisitions were reconstructed (decay and CT-based attenuation corrected) with filtered back projection (FBP) using a Ramp filter with a cutoff frequency of 0.5 mm^{-1}.

LPS and AMPA studies

[^{11}C]A-836339 dynamic PET scans were acquired 2 days (LPS) or 7 days (AMPA) after intrastriatal injection using a Siemens Inveon® small animal PET-CT scanner. Animals were anaesthetized with isoflurane (induction: 4%, maintenance: 2–2.5%) in oxygen. The radiolabeled compound was injected in the caudal vein through a 24 gauge catheter concomitantly with the beginning of the PET acquisition. The mean injected doses were ~40 MBq and PET data were acquired during 60 minutes. The acquisition protocol used the following parameters: the time coincidence window was set to 3,438 ns and the levels of energy discrimination were set to 350 and 650 keV. The list-mode acquired data files were histogrammed into 3-D sinograms with a maximum ring difference of 79 and span of 3. The list-mode data were sorted into 24 dynamic frames (3x30; 5x60; 5x120; 3x180; 3x240; 4x300 and 1x150 seconds). Finally, the emission sinograms (i.e. each frame) were normalized, corrected for scatter, attenuation and radioactivity decay and reconstructed using Fourier rebinning (FORE) and ordered subset expectation maximization (OSEM) 2D (16 subsets and 4 iterations). To acquire attenuation correction factors a CT (Inveon® PET-CT) or a transmission scan using an external ^{68}Ge point source (Inveon® PET) was performed immediately prior to the PET scan for each animal.

Positron emission tomography image analysis

Cerebral ischemia studies

PET images were analyzed using PMOD image analysis software (PMOD Technologies Ltd, Zürich, Switzerland). To verify the anatomical location of the signal, PET images were co-registered to the anatomical data of a MRI rat brain template. VOIs were manually drawn in the entire ipsilateral hemisphere that contained the territory irrigated by the middle cerebral artery on slices of a MRI (T_2W) rat brain template from the PMOD software to study the [^{11}C]A-836339 and [^{18}F]DPA-714 PET signal. For quantification of [^{11}C]A-836339, the simplified reference tissue model (SRTM) [32] from PMOD software was used to assess the BP_{ND} of the tracer to the tissue in the ischemic brain hemisphere. This model relies on a two-tissue reversible compartment for a target region (here ipsilateral brain hemisphere) and a single-tissue compartment for a reference region (here cerebellum). The BP values calculated by the simplified reference-tissue model are referred as BP_{ND} (non-displaceable), which is the BP of the tracer to the tissue and refers to ratio of specifically bound radioligand to that of non-displaceable radioligand in tissue at equilibrium. For quantification of [^{18}F]DPA-714 uptake, the last four frames in steady state were used to calculate the summed PET binding during the last 15 minutes of acquisition. PET signal uptake was averaged in each ROI and expressed as percentage of injected dose per cubic centimetre (%ID/cc).

LPS and AMPA studies

PET image analysis was performed using VINCI, a fast graphical image analysis package [33] with image co-registration tools. PET images were co-registered to an MRI template.[34] The Anatomist BrainVISA software package (http://www.brainvisa.info) was also used for data evaluation. For quantitative analysis a volume-of-interest (VOI) analysis was performed on kinetic image data sets. Two VOIs were manually delineated, one around the injection site in the ipsilateral (ipsilateral) and one control VOI in the contralateral hemisphere (contralateral). The time activity curves measured within these VOIs were finally obtained from dynamic PET data and were normalized for the injected dose.

Immunohistochemistry

Immunohistochemistry staining was performed at control (day 0), day 7 and day 28 after cerebral ischemia. Animals were terminally anesthetized, killed by decapitation; the brain was removed, frozen and cut in 5-μm-thick sections in a cryostat. Sections were fixed in acetone (−20°C) during 2 minutes, washed with phosphate-buffered saline (PBS), saturated with a solution of bovine serum albumin (BSA) 5% / Tween 0.5% in PBS during 15 minutes at room temperature, and incubated during 1 hour at room temperature with primary antibodies BSA (5%) / Tween (0.5%) in PBS. Sections were stained for CB2 with rabbit anti-rat CB2 (1:500, AbCam, Cambridge, UK) and for CD11b with mouse anti-rat CD11b (1:300; Serotec, Raleigh, NC, USA). Sections were washed (3 × 10 minutes) in PBS and incubated for 1 hour at room temperature with secondary antibodies Alexa Fluor 488 goat anti-rabbit IgG and Alexa Fluor 594 goat anti-mouse IgG (Molecular Probes, Life Technologies, Madrid, Spain, 1:1,000) in BSA 5%/Tween 0.5% in PBS, washed again (3 × 10 minutes) in PBS, and mounted with a prolong with DAPI antifade kit in slices (Molecular Probes Life Technologies, Madrid, Spain). Standardized images acquisition was performed with an Axio Observer Z1 (Zeiss, Le Pecq, France) equipped with a motorized stage.

Neurological assessment

The assessment of neurological outcome induced by cerebral ischemia was based on a previously reported 9-neuroscore test.[35] Four consecutive tests were performed on ischemic animals submitted to longitudinal imaging studies at 0, 1, 3, 7, 14, 21 and 28 days, and before (day 0) and at day 7 after ischemia in treated rats as follows: (a) spontaneous activity (moving and exploring = 0, moving without exploring = 1, no moving = 2); (b) left drifting during displacement (none = 0, drifting only when elevated by the tail and pushed or pulled = 1, spontaneous drifting = 2, circling without displacement or spinning = 3), (c) parachute reflex (symmetrical = 0, asymmetrical = 1, contralateral forelimb retracted = 2), and (d) resistance to left forepaw stretching (stretching not allowed = 0, stretching allowed after some attempts = 1, no resistance = 2). Total score could range from 0 (normal) to a 9 (highest handicap) point-scale.

Statistical analyses

Binding values within the ipsilateral hemisphere were averaged and compared with the averaged baseline control values (before MCAO) using one-way ANOVA analysis of variance followed by Dunnett's multiple comparison tests for post hoc analysis. An unpaired t-test was used to compare [^{11}C]A-836339 uptake values within the ipsilateral versus the contralateral hemisphere of LPS- and AMPA-injected animals, respectively. The effect of JWH133 in ischemic rats was compared to control infarcted rats using an unpaired t-test. Finally, neurological outcome comparisons before and at day 7 after ischemia were performed using Mann-Whitney U-test. The level of significance was regularly set at $p < 0.05$. Statistical analyses were performed with Graph Pad Prism software, version 5 (La Jolla, CA, USA).

RESULTS

[^{11}C]A-836339 PET after cerebral ischemia

The levels and distribution of cannabinoid CB2 receptors were explored by PET imaging after 90 minutes MCAO and 1-28 days reperfusion in rats. The coronal brain images with normalized color scale shown in Figure 1A-C illustrate the [^{11}C]A-836339-PET uptake signals in ischemic rats at control (day 0) and at 7, and 28 days after reperfusion (Figure 1A-C). The extent of brain damage after cerebral ischemia was assessed using T2W-MRI at 1 day after ischemia onset. Hyperintensities of T2W images showed similar infarct extents as well as locations affected. All ischemic rats subjected to nuclear imaging studies showed cortical and striatal MRI alterations (mean± s.d. 357.64 ± 45.47 mm^3, n=6). Quantification of the PET images provided information related to the time-course activity of CB2 receptors in the ipsilateral hemisphere at days 0 (control) and 1, 3, 7, 14, 21 and 28 days after MCAO (Figure 1D, n=6). In the infarcted hemisphere, the PET signal for [^{11}C]A-836339 showed a non-significant mild binding increase during the first week followed by an uptake decrease from days 14 to 28 after cerebral ischemia in rats (Figure 1D). The time-activity curves (TACs) generated in the ischemic cerebral hemisphere at days 0 and 7 after ischemia showed that [^{11}C]A-836339 uptake reached a peak value of radioactivity at few minutes after bolus injection followed by a fast wash-out during the following 15 minutes. Likewise, the radiotracer uptake reached a plateau level from 30 to 60 minutes after bolus injection. PET uptake at day 7 showed a non-significant difference in comparison to control animals (Figure 1E).

[^{11}C]A-836339 PET after LPS and AMPA injection

The levels and distribution of cannabinoid CB2 receptor were explored by PET imaging at days 2 and 7 after LPS (Figure 2) and AMPA (Figure 3) injection in rats, respectively. The coronal brain images with normalized color scale shown in Figures 2A and 3A display the [^{11}C]A-836339-PET uptake at day 2 after

LPS (Figure 2A) and day 7 after AMPA injection (Figure 3A). The TACs generated in the ipsilateral and contralateral striatum after LPS (Figure 2B, n=4) and AMPA (Figure 3B, n=2) injection showed a peak uptake of [^{11}C]A-836339 at few minutes after bolus injection followed by a fast wash-out later on. The results showed only low [^{11}C]A-836339 uptake after both LPS and AMPA injection in the injured striatum. Indeed, similar signal levels were observed in both ipsilateral and contralateral striatum after neuroinflammation induced by LPS and AMPA injection.

Expression of cannabinoid CB2 receptor in microglia after MCAO

Immunofluorescence staining exhibited CB2 expression in microglia/macrophages after ischemia (Figure 4). At day 7, cells with the morphology of amoeboid reactive microglia/macrophages showed intense CD11b immunoreactivity in the lesion (in red; Figure 4A) followed by a decrease at day 28 (in red; Figure 4A). In contrast, CB2 receptor immunoreactivity showed a mild increase at day 7 followed by a decrease at day 28 after cerebral ischemia (in green; Figure 4B). DAPI labeling displayed similar cellular density before and after MCAO (in blue; Figure 4C). The over-reactivity of microglia co-localized partially with the cellular expression of CB2 receptor at days 7 and 28 after ischemia (in red and green; Figure 4D).

Effect of CB2 receptor activation on neuroinflammation following cerebral ischemia

The effect of CB2 receptor activation with JWH133 on neuroinflammation was explored by PET imaging of TSPO with [^{18}F]DPA-714 at day 7 following MCAO (Figure 5). All the images were quantified in standard units, i.e., %ID/cc. Coronal and axial images with normalized color scale illustrate the [^{18}F]DPA-714 PET uptake in vehicle (MCAO) (Figure 5A and B) and JWH133 (MCAO+ JWH133) (Figure 5C and

D) ischemic rats. JWH133 treatment evidenced a significant decrease of [^{18}F]DPA-714 binding in the ischemic cerebral hemisphere in relation to non-treated ischemic rats (P<0.05, Figure 5G). Neurological score at day 1 after ischemia showed similar values reflecting that the groups presented similar neurological impairment before the start of the treatments (Figure 5H). At day 7, ischemic rats treated with JWH133 displayed a similar neurofunctional improvement in relation to that showed by non-treated ischemic rats (P<0.01, Figure 5H).

DISCUSSION

During the last years, cannabinoid CB2 receptors have emerged as promising targets for the diagnosis and therapy of neurologic and neurodegenerative pathologies. Preclinical studies have evidenced that the cannabinoid receptor system might exert a neuroprotective effect over a large number of neurologic and neurodenerative disorders.[8-18] Despite this, the application of cannabinoid-based medicines into the clinical use is still the major challenge for the near future. The evaluation of promising novel radiotracers for the *in vivo* imaging of CB2 receptors may be essential to better understand the role of CB2R in cerebral inflammation. Because of this, we have monitored the *in vivo* expression of CB2 receptors with [^{11}C]A-836339 PET after cerebral ischemia and in two rat models of neuroinflammation such as, intrastriatal LPS and AMPA injection, in combination with inmunohistochemistry.

PET imaging of CB2 receptors with [^{11}C]A-836339

PET imaging studies with [^{11}C]A-836339 have demonstrated a low background uptake in the normal mouse brain that might improve the visualization of the CB2 receptor expression after a neuroinflammatory reaction.[22] These findings are consistent with the low [^{11}C]A-836339 PET binding observed in the control (day 0) rat brain before cerebral ischemia (Figure 1A). In the present study, [^{11}C]A-836339 was evaluated from day 1 to day 28 after cerebral ischemia to monitor CB2 expression under neuroinflammatory conditions. In the infarcted cerebral hemisphere, [^{11}C]A-836339 showed a non-significant binding potential increase at day 7 after reperfusion followed by a BP_{ND} recovery to pseudo-control values at days 14 to 28 after ischemia (Figure 1D). This result is also reflected in the marginally increased time activity curve of [^{11}C]A-836339 uptake (%ID/cc) in the ipsilateral hemisphere at day 7 in comparison to the control rat brain (Figure 1E). Altogether, these findings stand in agreement with Vandeputte and collaborators who, after monitoring CB2 receptors with [^{11}C]NE40 PET following a photothrombotic stroke model, did not observe any significant difference between stroke and sham-operated animals.[24] In fact, these previous results may be explained by the relatively low affinity of

[^{11}C]NE40 (*K*i 9.6 nM) that might limit its sensitivity for the detection of low concentration of CB2 receptors.[24] [^{11}C]A-836339 displays a significantly higher binding affinity (*K*i 0.7 nM) than [^{11}C]NE40.[22] Our negative results in the ischemic model suggest that CB2 receptor radioligands with subnanomolar affinity might be required to properly map these receptors in small rodents with PET imaging. In view of the negative results obtained for the ischemic rat model, two acute models of neuroinflammation such as intrastriatal injection of LPS and AMPA were used to support our findings. [^{11}C]A-836339 PET images did not show any significant binding increase in the injured striatum after LPS (Figure 2) and AMPA (Figure 3) administration in relation to the non-lesioned brain hemisphere. Nevertheless, these results stand in contrast with those shown by Horti and collaborators who observed specific cerebral [^{11}C]A-836339 PET uptake in the LPS-induced mouse model of neuroinflammation.[22] These differences could be explained by the use of different LPS-treatment dose and protocols; while a single intraperitoneal LPS injection of circa 125 μg was chosen by Horti and colleagues, a 1 μg intracerebral LPS injection was used in our study. Nevertheless, as described by Dickens and colleagues[26] this low dose for intrastriatal LPS injection is sufficient to create a neuroinflammatory lesion that can be monitored using TSPO PET radioligands.

***Ex vivo* CB2 expression after cerebral ischemia**

Immunohistochemistry confirmed the activation of microglia at day 7 followed by a decrease at day 28 after ischemia onset. These findings confirmed the well-known neuroinflammatory response after 90 min-MCAO in rats.[28] Further, CB2 receptors displayed an expression increase, albeit modest, one week after reperfusion followed by a reduction during the following weeks (Figure 4). Likewise, these results confirmed that microglia/macrophages partially co-localized with CB2 receptor after cerebral ischemia in rats. Indeed, the low CB2 receptor expression after cerebral ischemia stand in accordance with the lack of specific [^{11}C]A-836339 uptake following experimental stroke in rats. In addition, the low CB2 receptor expression levels after cerebral ischemia has been previously observed during the three days following a photothrombotic model of ischemic stroke in mice. [24]

CB2 activation attenuates neuroinflammatory response after cerebral ischemia.

Pharmacologic CB2 receptor activation with the selective agonists JWH133, O-3853 and O-1966 has been associated with (i) the reduction of white blood cells in both rolling and adhesion to the cerebral vessels, (ii) a decrease of brain lesion size and (iii) the improvement of motor function after cerebral ischemia in mice [8, 10, 36, 37]. In our study, we explored the effect of JWH133 on neuroinflammation by using [^{18}F]DPA-714 PET binding following cerebral ischemia (Figure 5). The activation of CB2 receptors with JWH133 induced a significant decrease of the TSPO expression following seven days after reperfusion (Figure 5G). Thus, these results support the role of CB2 receptor on inflammatory reaction following cerebral ischemia in rats. Despite these findings, the treatment with CB2 receptor agonist did not evidence a neurological handicap improvement at day 7 after reperfusion in relation to the non-treated rats.

Summary and conclusions

We report here [^{11}C]A-836339 PET imaging to assess CB2 receptor expression following cerebral ischemia, LPS and AMPA induced models of neuroinflammation and its relationship with inflammatory response after cerebral ischemia in rats. Our results showed a lack of [^{11}C]A-836339 uptake after stroke, LPS and AMPA injection evidencing the limitation of this radiotracer to image CB2 receptor under pathologic conditions in brain. Besides, CB2 receptor displayed a modest expression increase after cerebral ischemia by using immunohistochemistry and the activation of CB2 receptors was able to promote a decrease of [^{18}F]DPA-714 uptake. Therefore, these findings provide novel insights on the usefulness of [^{11}C]A-836339 to monitor *in vivo* CB2 receptor expression by using PET imaging. Future studies will have to investigate alternative radiotracers with higher sensitivity that could provide an accurate binding of CB2 receptor following brain inflammation.

Acknowledgements

The authors would like to thank B. Sczcupak, L. Morales, A Leukona, V. Salinas, A Arrieta and A Cano for technical support in the radiosynthesis and technical assistance in the PET studies, and the Department of Industry of the Basque Government and Spanish Ministry of Economy and Competitiveness through grant SAF2014-54070-JIN for financial support. This research was partly funded by the EU 7th Framework Programme (FP7/2007-2013) under grant agreement n° 278850 (INMiND) as well as France Life Imaging under grant agreement ANR-11-INBS-0006 (FLI).

Declaration of conflicting interests

The author(s) declared no potential conflicts of interest with respect to the research, authorship, and/or publication of this article.

Author's contributions

GP, VG-V, DP, AM performed experiments, RB, FD, JLL, AW, AM, designed experiments, AW, AM, FD analyzed data and prepared the manuscript.

BIBLIOGRAPHY

1. Manzanares J, Julian M and Carrascosa A. Role of the cannabinoid system in pain control and therapeutic implications for the management of acute and chronic pain episodes. *Curr Neuropharmacol*. 2006; 4: 239-57.
2. Fernandez-Ruiz J, Moro MA and Martinez-Orgado J. Cannabinoids in Neurodegenerative Disorders and Stroke/Brain Trauma: From Preclinical Models to Clinical Applications. *Neurotherapeutics*. 2015; 12: 793-806.
3. Mackie K. Distribution of cannabinoid receptors in the central and peripheral nervous system. *Handb Exp Pharmacol*. 2005; 168: 299-325.
4. Cabral GA, Raborn ES, Griffin L, Dennis J and Marciano-Cabral F. CB2 receptors in the brain: role in central immune function. *Br J Pharmacol*. 2008; 153: 240-51.
5. Miller AM and Stella N. CB2 receptor-mediated migration of immune cells: it can go either way. *Br J Pharmacol*. 2008; 153: 299-308.
6. Stella N. Cannabinoid and cannabinoid-like receptors in microglia, astrocytes, and astrocytomas. *Glia*. 2010; 58: 1017-30.
7. Matias I, Pochard P, Orlando P, Salzet M, Pestel J and Di Marzo V. Presence and regulation of the endocannabinoid system in human dendritic cells. *Eur J Biochem*. 2002; 269: 3771-8.
8. Zarruk JG, Fernandez-Lopez D, Garcia-Yebenes I, et al. Cannabinoid type 2 receptor activation downregulates stroke-induced classic and alternative brain macrophage/microglial activation concomitant to neuroprotection. *Stroke*. 2012; 43: 211-9.
9. Nagayama T, Sinor AD, Simon RP, et al. Cannabinoids and neuroprotection in global and focal cerebral ischemia and in neuronal cultures. *J Neurosci*. 1999; 19: 2987-95.
10. Zhang M, Martin BR, Adler MW, Razdan RK, Jallo JI and Tuma RF. Cannabinoid CB(2) receptor activation decreases cerebral infarction in a mouse focal ischemia/reperfusion model. *J Cereb Blood Flow Metab*. 2007; 27: 1387-96.
11. Kong W, Li H, Tuma RF and Ganea D. Selective CB2 receptor activation ameliorates EAE by reducing Th17 differentiation and immune cell accumulation in the CNS. *Cell Immunol*. 2014; 287: 1-17.
12. Arevalo-Martin A, Molina-Holgado E and Guaza C. A CB(1)/CB(2) receptor agonist, WIN 55,212-2, exerts its therapeutic effect in a viral autoimmune model of multiple sclerosis by restoring self-tolerance to myelin. *Neuropharmacology*. 2012; 63: 385-93.
13. Aso E, Juves S, Maldonado R and Ferrer I. CB2 cannabinoid receptor agonist ameliorates Alzheimer-like phenotype in AbetaPP/PS1 mice. *J Alzheimers Dis*. 2013; 35: 847-58.
14. Palazuelos J, Aguado T, Pazos MR, et al. Microglial CB2 cannabinoid receptors are neuroprotective in Huntington's disease excitotoxicity. *Brain*. 2009; 132: 3152-64.
15. Sagredo O, Gonzalez S, Aroyo I, et al. Cannabinoid CB2 receptor agonists protect the striatum against malonate toxicity: relevance for Huntington's disease. *Glia*. 2009; 57: 1154-67.
16. Price DA, Martinez AA, Seillier A, et al. WIN55,212-2, a cannabinoid receptor agonist, protects against nigrostriatal cell loss in the 1-methyl-4-phenyl-1,2,3,6-tetrahydropyridine mouse model of Parkinson's disease. *Eur J Neurosci*. 2009; 29: 2177-86.
17. Shoemaker JL, Seely KA, Reed RL, Crow JP and Prather PL. The CB2 cannabinoid agonist AM-1241 prolongs survival in a transgenic mouse model of amyotrophic lateral sclerosis when initiated at symptom onset. *J Neurochem*. 2007; 101: 87-98.

18. Kim K, Moore DH, Makriyannis A and Abood ME. AM1241, a cannabinoid CB2 receptor selective compound, delays disease progression in a mouse model of amyotrophic lateral sclerosis. *Eur J Pharmacol*. 2006; 542: 100-5.
19. Mu L, Bieri D, Slavik R, et al. Radiolabeling and in vitro /in vivo evaluation of N-(1-adamantyl)-8-methoxy-4-oxo-1-phenyl-1,4-dihydroquinoline-3-carboxamide as a PET probe for imaging cannabinoid type 2 receptor. *J Neurochem*. 2013; 126: 616-24.
20. Slavik R, Herde AM, Bieri D, et al. Synthesis, radiolabeling and evaluation of novel 4-oxo-quinoline derivatives as PET tracers for imaging cannabinoid type 2 receptor. *Eur J Med Chem*. 2015; 92: 554-64.
21. Saccomanni G, Pascali G, Carlo SD, et al. Design, synthesis and preliminary evaluation of (18)F-labelled 1,8-naphthyridin- and quinolin-2-one-3-carboxamide derivatives for PET imaging of CB2 cannabinoid receptor. *Bioorg Med Chem Lett*. 2015; 25: 2532-5.
22. Horti AG, Gao Y, Ravert HT, et al. Synthesis and biodistribution of [11C]A-836339, a new potential radioligand for PET imaging of cannabinoid type 2 receptors (CB2). *Bioorg Med Chem*. 2010; 18: 5202-7.
23. Ahmad R, Koole M, Evens N, et al. Whole-body biodistribution and radiation dosimetry of the cannabinoid type 2 receptor ligand [11C]-NE40 in healthy subjects. *Mol Imaging Biol*. 2013; 15: 384-90.
24. Vandeputte C, Casteels C, Struys T, et al. Small-animal PET imaging of the type 1 and type 2 cannabinoid receptors in a photothrombotic stroke model. *Eur J Nucl Med Mol Imaging*. 2012; 39: 1796-806.
25. Martin A, Boisgard R, Theze B, et al. Evaluation of the PBR/TSPO radioligand [(18)F]DPA-714 in a rat model of focal cerebral ischemia. *J Cereb Blood Flow Metab*. 2010; 30: 230-41.
26. Dickens AM, Vainio S, Marjamaki P, et al. Detection of microglial activation in an acute model of neuroinflammation using PET and radiotracers 11C-(R)-PK11195 and 18F-GE-180. *J Nucl Med*. 2014; 55: 466-72.
27. Chauveau F, Van Camp N, Dolle F, et al. Comparative evaluation of the translocator protein radioligands 11C-DPA-713, 18F-DPA-714, and 11C-PK11195 in a rat model of acute neuroinflammation. *J Nucl Med*. 2009; 50: 468-76.
28. Martin A, Szczupak B, Gomez-Vallejo V, et al. In vivo PET imaging of the alpha4beta2 nicotinic acetylcholine receptor as a marker for brain inflammation after cerebral ischemia. *J Neurosci*. 2015; 35: 5998-6009.
29. Justicia C, Perez-Asensio FJ, Burguete MC, Salom JB and Planas AM. Administration of transforming growth factor-alpha reduces infarct volume after transient focal cerebral ischemia in the rat. *J Cereb Blood Flow Metab*. 2001; 21: 1097-104.
30. Kuhnast B, Damont A, Hinnen F, et al. [18F]DPA-714, [18F]PBR111 and [18F]FEDAA1106-selective radioligands for imaging TSPO 18 kDa with PET: automated radiosynthesis on a TRACERLAb FX-FN synthesizer and quality controls. *Appl Radiat Isot*. 2012; 70: 489-97.
31. Damont A, Hinnen F, Kuhnast B, et al. Radiosynthesis of [18F]DPA-714, a selective radioligand for imaging the translocator protein (18 kDa) with PET. *Journal of Labelled Compounds and Radiopharmaceuticals*. 2008; 51: 286-92.
32. Lammertsma AA and Hume SP. Simplified reference tissue model for PET receptor studies. *Neuroimage*. 1996; 4: 153-8.
33. Cizek J, Herholz K, Vollmar S, Schrader R, Klein J and Heiss WD. Fast and robust registration of PET and MR images of human brain. *Neuroimage*. 2004; 22: 434-42.
34. Papp EA, Leergaard TB, Calabrese E, Johnson GA and Bjaalie JG. Waxholm Space atlas of the Sprague Dawley rat brain. *Neuroimage*. 2014; 97: 374-86.
35. Menzies SA, Hoff JT and Betz AL. Middle cerebral artery occlusion in rats: a neurological and pathological evaluation of a reproducible model. *Neurosurgery*. 1992; 31: 100-6.

36. Murikinati S, Juttler E, Keinert T, et al. Activation of cannabinoid 2 receptors protects against cerebral ischemia by inhibiting neutrophil recruitment. *Faseb J*. 2010; 24: 788-98.
37. Zhang M, Adler MW, Abood ME, Ganea D, Jallo J and Tuma RF. CB2 receptor activation attenuates microcirculatory dysfunction during cerebral ischemic/reperfusion injury. *Microvasc Res*. 2009; 78: 86-94.

FIGURE LEGENDS

Figure legends

Figure 1.Time course of the progression of [^{11}C]A-836339 signal before and after middle cerebral artery occlusion (MCAO). Serial CB2 receptors PET binding images of coronal planes at control (day 0) (A), day 7 (B) and day 28 (C) after reperfusion. PET images are co-registered with a MRI (T_2W) template to localize the PET signal. Images correspond to the lesion evolution of the same animal over time. (D) BP_{ND} (mean ±SD) of [^{11}C]A-836339 was quantified in the entire ipsilateral cerebral hemisphere. The upper right panel show the selected brain ROI for the quantification defined on a slice of a MRI (T2W) template. Rats (n=6) were repeatedly examined by PET before (day 0) and at 1, 3, 7, 14, 21 and 28 after ischemia. (E) Time activity curves of [^{11}C]A-836339 binding in the ipsilateral hemisphere at days 0 and 7 following cerebral ischemia.

Figure 2. CB2 receptor binding with [^{11}C]A-836339 PET at day 2 after LPS administration. (A) [^{11}C]A-836339 PET image is co-registered with a MRI (T_2W) template to localize the PET signal. (B) Average time activity curves of [^{11}C]A-836339 binding at day 2 for VOIs placed in the ipsilateral and contralateral striatums after LPS injection.

Figure 3. CB2 receptor binding with [^{11}C]A-836339 PET at day 7 after AMPA administration. (A) [^{11}C]A-836339 PET image is co-registered with a MRI (T_2W) template to localize the PET signal. (B) Average time activity curves of [^{11}C]A-836339 binding at day 7 for VOIs placed in the ipsilateral and contralateral striatums after AMPA injection.

Figure 4. Immunofluorescent labeling of CD11b (red), CB2 (green), and DAPI (blue) in the ischemic area, shown as three channels. The data show temporal evolution of microglia expressing CB2 at day 0 (control) (left column), day 7 (middle column) and day 28 (right column) after ischemia. (A) CD11b-reactive microglia/macrophages increase at days 7 to 28 (B) corresponding to the temporal CB2 immunoreactivity after ischemia (B). (C) DAPI labeling evidence similar cellular density before and after MCAO. (D) Merged images of three immunofluorescent channels at different time points. Scale bars, 20 μm.

Figure 5. Normalized coronal (A, C) and axial (B, D) PET images of [^{18}F]DPA-714 at day 7 after middle cerebral artery occlusion (MCAO) in vehicle (A, B) and JWH133 (C, D) rats. PET images are co-registered with a MRI (T_2W) rat template to localize anatomically the PET signal. [^{18}F]DPA-714 uptake was quantified as %ID/cc (mean ± SD) in the entire ipsilateral cerebral hemisphere. Vehicle (n=5) and JWH133 (n=7) were examined by PET at 7 days after ischemia (G). The neurologic score shows similar neurologic outcome at day 1 after ischemia (before the start of treatment) followed by a neurological outcome improvement at day 7 after cerebral ischemia (H). *p<0.05 compared with vehicle; $^{\#\#}p$<0.01 compared with day 1.

Figure 1

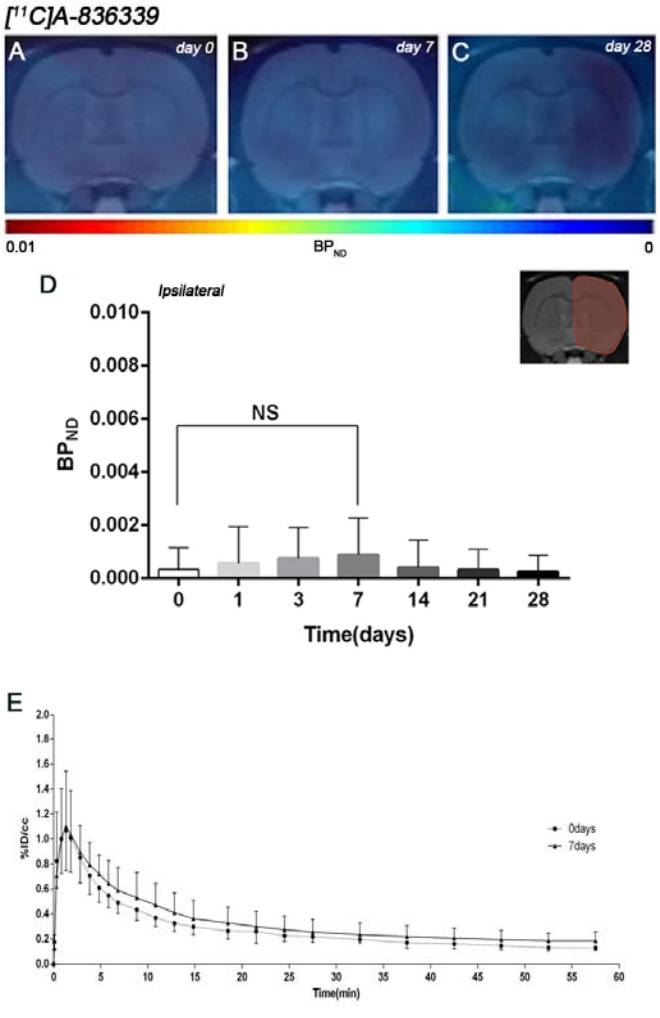
[11C]A-836339
A
day 0
B
day 7
C
day 28
0.01
BPND
0
D
Ipsilateral
0.010
0.008
0.006
0.004
0.002
0.000
BPND
NS
0
1
3
7
14
21
28
Time(days)
E
%ID/cc
0days
7days
Time(min)

Figure 2

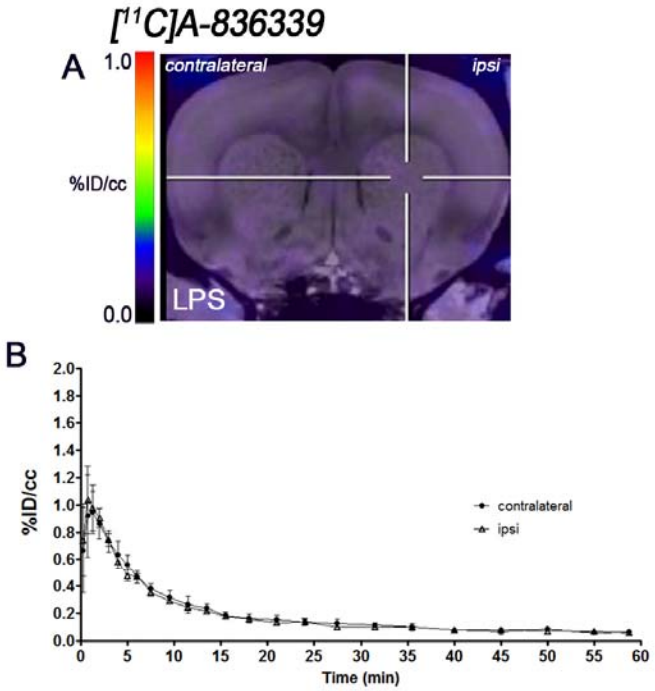
[11C]A-836339
A
1.0
%ID/cc
0.0
contralateral
ipsi
LPS
B
%ID/cc
2.0
1.8
1.6
1.4
1.2
1.0
0.8
0.6
0.4
0.2
0.0
0
5
10
15
20
25
30
35
40
45
50
55
60
Time (min)
contralateral
ipsi

Figure 3

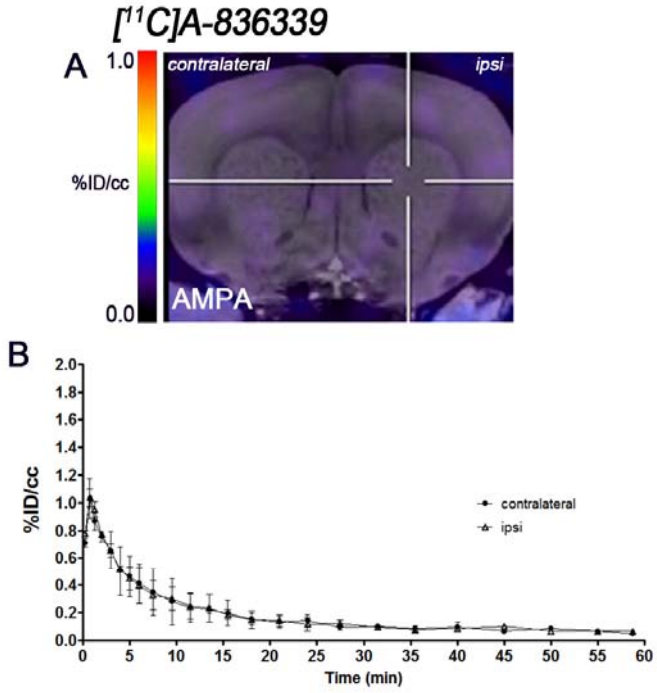
[11C]A-836339
A
1.0
%ID/cc
0.0
contralateral
ipsi
AMPA
B
%ID/cc
2.0
1.8
1.6
1.4
1.2
1.0
0.8
0.6
0.4
0.2
0.0
0
5
10
15
20
25
30
35
40
45
50
55
60
Time (min)
contralateral
ipsi

Figure 4

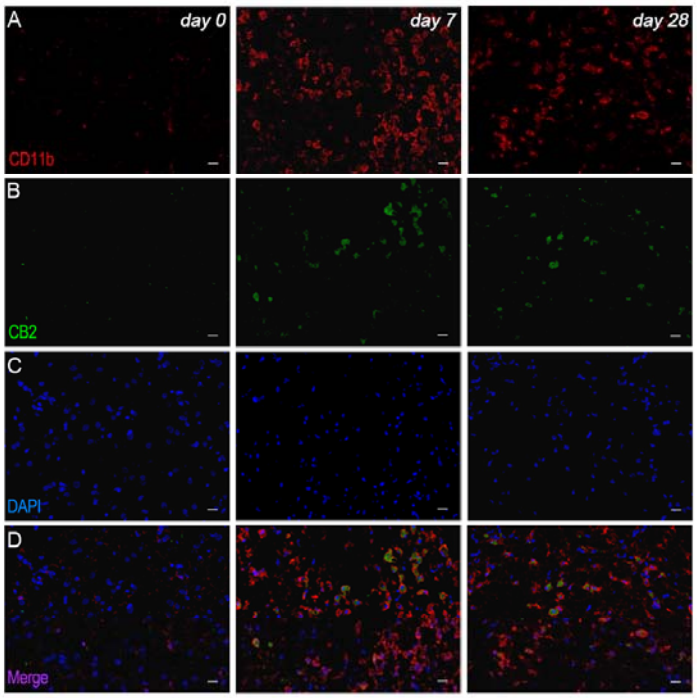

Figure 5

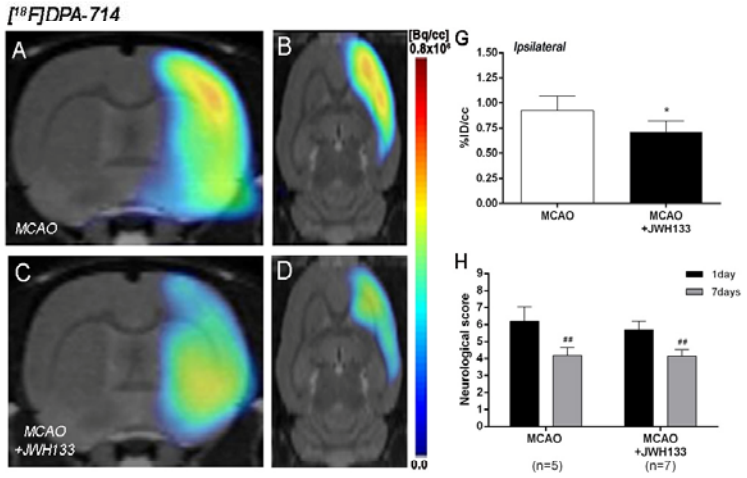
[18F]DPA-714
A
B
C
D
MCAO
MCAO
+JWH133
[Bq/cc]
0.8x10⁶
0.0
G
Ipsilateral
%ID/cc
1.50
1.25
1.00
0.75
0.50
0.25
0.00
*
MCAO
MCAO
+JWH133
H
Neurological score
1day
7days
##
##
MCAO
(n=5)
MCAO
+JWH133
(n=7)